International Journal of Crashworthiness
Publication details, including instructions for authors and subscription information:
http://www.tandfonline.com/loi/tcrs20

Increasing automobile crash response metamodel accuracy through adjusted cross validation error based on outlier analysis

Erdem Acar[a]
[a] Department of Mechanical Engineering, TOBB University of Economics and Technology, Ankara, Turkey
Published online: 19 Nov 2014.

To cite this article: Erdem Acar (2015) Increasing automobile crash response metamodel accuracy through adjusted cross validation error based on outlier analysis, International Journal of Crashworthiness, 20:2, 107-122, DOI: 10.1080/13588265.2014.977839

To link to this article: http://dx.doi.org/10.1080/13588265.2014.977839

International Journal of Crashworthiness, 2015
Vol. 20, No. 2, 107–122, http://dx.doi.org/10.1080/13588265.2014.977839

Increasing automobile crash response metamodel accuracy through adjusted cross validation error based on outlier analysis

Erdem Acar*

Department of Mechanical Engineering, TOBB University of Economics and Technology, Ankara, Turkey

(*Received 11 August 2014; accepted 14 October 2014*)

Automakers spread on effort to maintain the crashworthiness of vehicle structures while aiming to reduce their weight. Substantial weight savings can be obtained by vehicle redesign through optimisation. Finite element based crashworthiness simulation models have contributed greatly to the optimisation of vehicle structures. These high-fidelity crash simulations may be performed many times during optimisation, thereby making optimisation studies computationally intractable. Metamodels (surrogate models) that can mimic the behaviour of the crash simulation models emerge as a solution to the computational burden. Prediction capability in metamodelling can be improved by combining many different metamodels in the form of an ensemble model. In this paper, approaches based on outlier analysis of cross validation errors are proposed to increase the accuracy of ensemble models constructed for crash response predictions. Full frontal and offset frontal crash response predictions of a c-class passenger car is used for demonstration, and it is found that the proposed approach reduces the metamodelling errors up to 12% and on average by about 4.5%.

Keywords: automobile; crash; cross validation; metamodel; outlier; surrogate model

Nomenclature

ENS:	ensemble of metamodels based on minimisation of $RMSE_{cv}$
ENSa:	ensemble of metamodels based on minimisation of adjusted $RMSE_{cv}$
KR0, KR1:	Kriging models constructed by using zeroth-order and first-order trend models, respectively
MSE:	mean square error (computed at test points)
MSE_{cv}:	mean square cross validation error (computed at training points)
N_M:	number of individual metamodels contributing to the ensemble
PRS2:	polynomial response surface of the second order
RBFm, RBFi:	radial basis functions constructed by using multiquadric and inverse multiquadric basis functions, respectively
RMSE:	root mean square error
$RMSE_{cv}$:	root mean square cross validation error
w_i:	contribution of the ith metamodel in the ensemble
$\hat{y}_{ens}$:	prediction of response obtained from the ensemble model
$\hat{y}_i$:	prediction of response obtained from the ith metamodel of the ensemble

1. Introduction

Occupant safety is a major concern in vehicle design. According to the National Highway Traffic Safety Administration, more than 33,000 people were killed and over 2.3 million others were injured in motor vehicle crashes in the United States in the year 2012 [6]. The initial impact point in fatal crashes for passenger vehicles is found to be frontal in 55% and side impact in 26% of the fatalities [5]. Meanwhile, the customers are attracted to the lightweight automobiles due to fuel economy considerations. For every 100 kg of weight reduction, the adjusted combined city/highway fuel consumption reduces by 0.31 L/100 km for a medium size car, and by 0.36 L/100 km for a light truck [11]. Therefore, the automakers spread on effort to maintain the crashworthiness of vehicle structures while aiming to reduce their weight.

Weight reduction of a vehicle can be achieved by material substitution [15,31,44,57] and vehicle redesign [7,14,19,29,30,35,61,62]. Material substitution aims to replace heavier iron and steel with lightweight aluminium, magnesium, high-strength steel, and plastics/composites. Vehicle redesign is usually achieved through topology, shape and size optimisation techniques. In addition, a successful combination of these material substitution and vehicle redesign through optimisation can lead to further weight reduction [27,32,42].

*Email: acar@etu.edu.tr

Finite element based crashworthiness simulation models have contributed greatly to the optimisation of vehicle structures. These simulation models are used in place of physical experiments and the crash responses of interest are predicted. Despite the huge progress in computational power and memory, high-fidelity crash simulations are still computationally expensive. In addition, these high-fidelity crash simulations may be performed many times during optimisation (hundreds or thousands of times depending on the problem size and the optimisation method selected); hence, the use of metamodels (surrogate models) that can mimic the behaviour of the crash simulation models emerge as a solution to the computational burden.

In literature, many different metamodelling methods have been used to estimate critical vehicle crash responses. These studies include but not limited to the use of polynomial response surface approximations [13,23,53,60], radial basis functions [1,17,18,25], Kriging [21, 33, 45] and others [38,40,54]. There is no consensus on the most accurate metamodel type for crashworthiness response prediction. In addition, it is also difficult for an analyst to know which metamodel type is the most accurate for a specific crash response for a specific crash scenario. Even though the traditional practice is to construct many different types of metamodels and select the most accurate one, there exist other studies that focus on merging multiple metamodels into a weighted average ensemble of metamodels for crash response prediction [4,20,39,63].

The contribution of each metamodel in the ensemble can be determined such that the mean square cross validation error (MSE_{cv}) is minimised with an aim to minimise the actual mean square error (MSE_{act}), because there is a strong positive correlation between the MSE_{cv} and MSE_{act}. In this paper, two approaches based on outlier analysis are proposed for improving the correlation between the cross validation error and actual error, and thereby increasing the accuracy of response predictions. The first approach is to remove outliers in the cross validation error set while computing the MSE_{cv}, and the second approach is to weigh down the outliers in the cross validation error set. In both approaches, an adjusted MSE_{cv} is obtained.

The paper is structured as follows. The automobile crash problem is defined in Section 2. The metamodel types used in this study are introduced in Section 3. Construction of ensemble of metamodels is discussed in Section 4. The details of adjusted cross validation error based on outlier analysis are given in Section 5. The results of this study are presented and discussed in Section 6. Finally, a list of important conclusions drawn from this study is presented in Section 7.

2. Problem definition

A modified version of the full scale finite element (FE) model of a c-class passenger car developed by the Partnership of a New Generation of Vehicles group [43] is used in this study. In the FE model (see Figure 1), 313 components are included with an overall mass of approximately 1210 kg. The FE model consists of 184,436 nodes and 179,844 elements, mostly Belytschko–Tsay shell elements. The total degrees of freedom in the FE model is over 1.1 million. Isotropic materials with the non-linear behaviour of material defined by the true stress–strain curves at different strain rates are used in the FE model. The crash simulations are performed using LS-DYNA. This crash problem is also used in an earlier study [1].

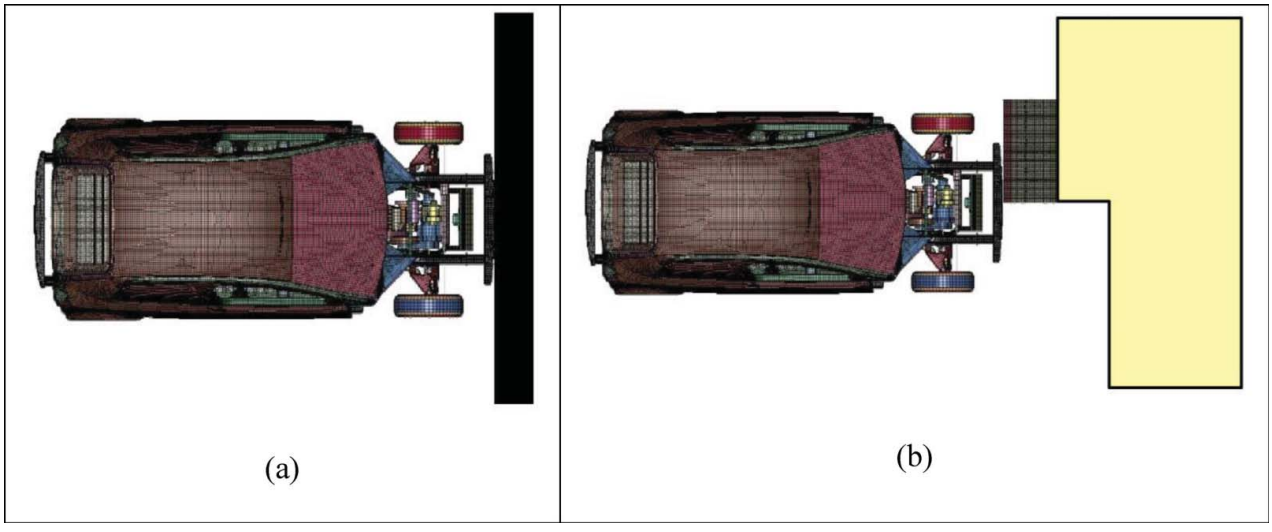

Figure 1. The FE model used in (a) full frontal impact and (b) offset frontal impact scenarios.

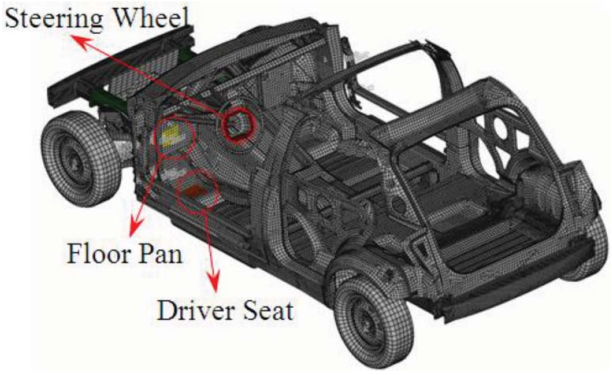

Figure 2. Vehicle FE model showing the side rail and locations of measured responses.

Table 1. The lower and upper bounds of the input variables.

Variable name	Symbol	Lower bound	Upper bound
Shape control parameters	x_1-x_4	−0.25	+0.25
Wall thickness of the side rails	x_5	0.75 mm	1.25 mm
Variability in the material stress−strain curve	x_6	−10%	+10%
Offset distance	x_7	20%	60%
Impact speed	x_8	14.60 m/s	16.70 m/s
Occupant mass	x_9	45.4 kg	136.2 kg

Full frontal impact (FFI) and offset frontal impact (OFI) scenarios are considered in this study (see Figure 1), whereas other possible scenarios such as side impact, roof crush and rear impact are not included. The vehicle crashes into a rigid wall in FFI scenario, whereas it collides with a deformable barrier that is placed in front of a rigid wall in OFI scenario.

The critical crash responses are chosen as the intrusion distances at the floor pan, the driver seat and steering-wheel locations (see Figure 2) corresponding to FFI and OFI scenarios, for a crash duration of 100 ms. Therefore, a total of six critical crash responses are considered. The crashworthiness of the vehicle can be improved by adjusting the geometric parameters of the two side rails that absorb the kinetic energy in a crash (see Figure 3). In the metamodelling study, the critical crash responses are related to the five geometric parameters of the side rails along with four random variables that capture variability in stress−strain curve, offset distance, impact speed and occupant mass (see Table 1). Therefore, the total number of input variables for the metamodels is nine. The effects of the first four design variables on the side rail geometry are depicted in Figure 4.

3. Metamodels

Metamodels (surrogate models) are approximate mathematical models that can mimic the behaviour of computationally expensive high-fidelity simulations. There exists a large number of metamodelling methods developed in literature. The commonly used metamodel types include the polynomial response surface approximations, PRS [9,37], Kriging, KR [49,51], radial basis functions, RBF [10,16], Gaussian process, GP [36,47], neural networks [8,52] and support vector regression, SVR [12,24]. A good review of metamodelling methods can be obtained from [46,59]. PRS, RBF and KR metamodels and the ensemble models composed of these metamodels are considered in this study.

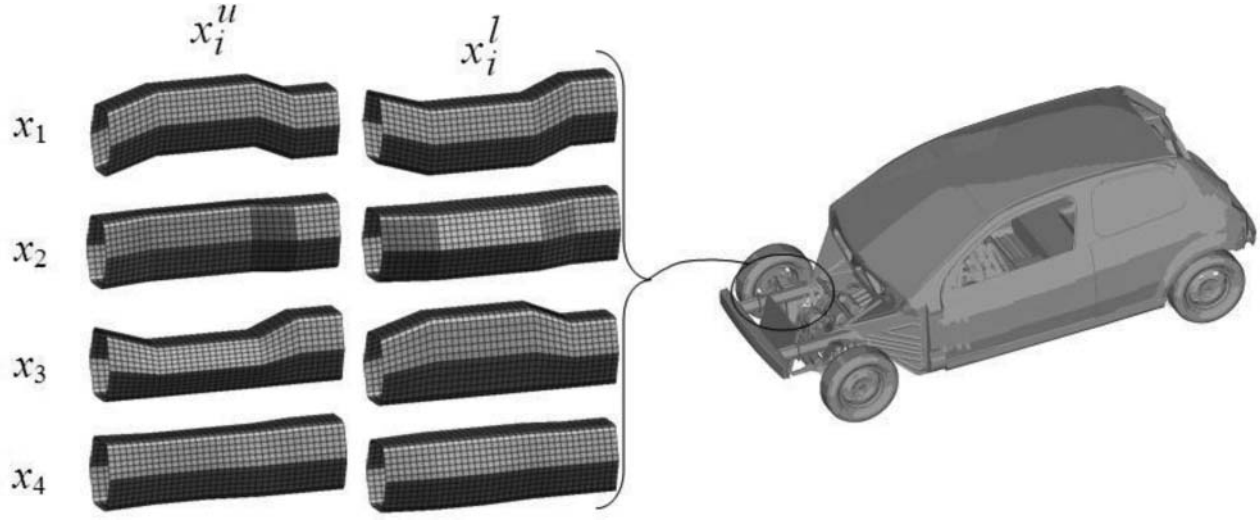

Figure 3. Geometry of the side rails corresponding to the upper and lower limits of the first four design variables.

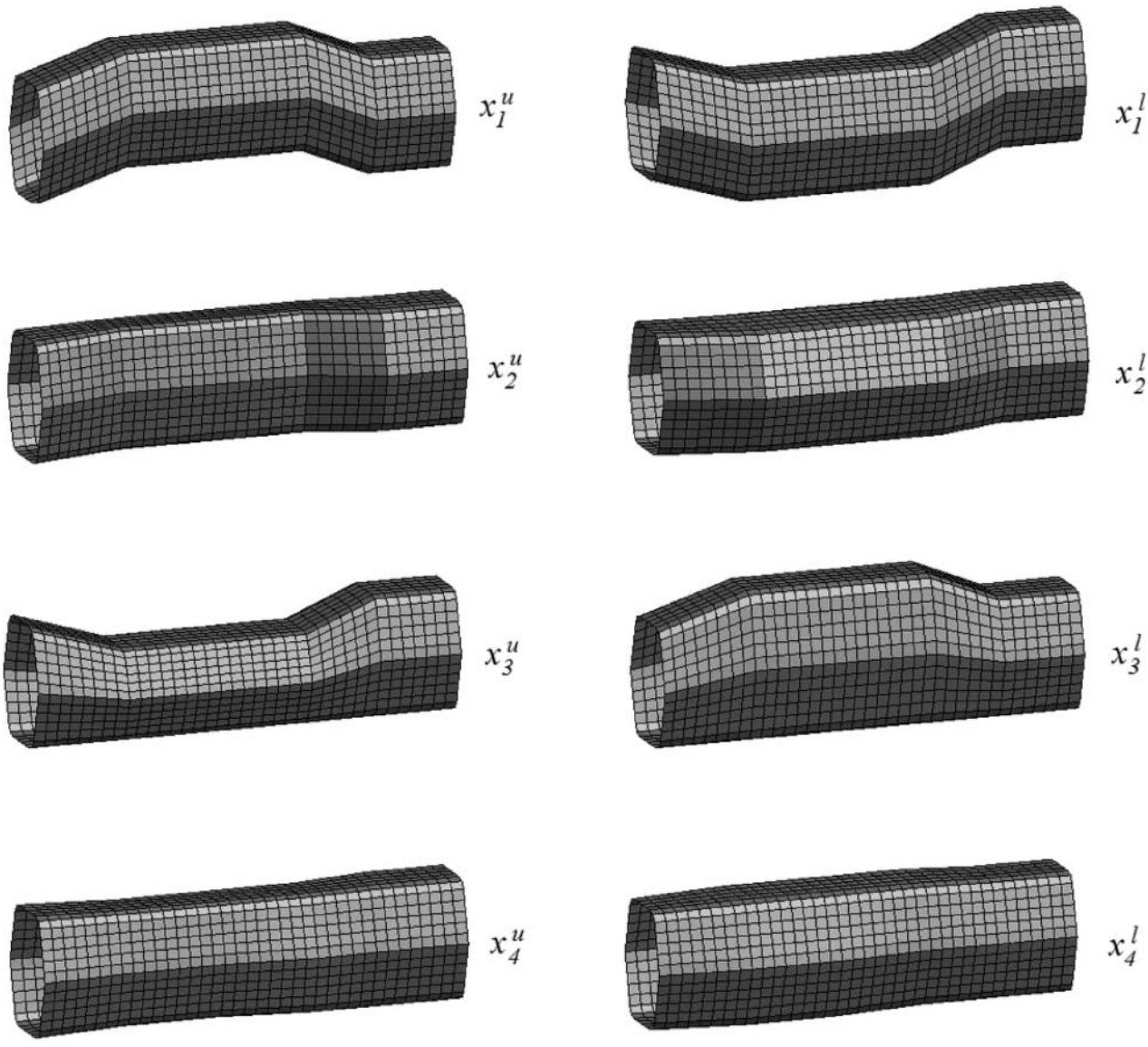

Figure 4. The effects of the first four design variables on the side rail geometry.

3.1. Polynomial response surface approximations, PRS

The most commonly used PRS model is the quadratic function with all terms included

$$\hat{y}(\mathbf{x}) = b_0 + \sum_{i=1}^{N_v} b_i x_i + \sum_{i=1}^{N_v} b_{ii} x_i^2 + \sum_{i=1}^{N_v - 1} \sum_{j=i+1}^{N_v} b_{ij} x_i x_j \quad (1)$$

where $\hat{y}(\mathbf{x})$ is the response surface approximation of the actual response function, $y(\mathbf{x})$, N_v is the number of variables in the input vector $\mathbf{x}$. The unknown coefficients b_0, b_i, b_{ii}, b_{ij} are determined through least squares fitting.

3.2. Radial basis function, RBF

RBF methods approximate the true function $y(\boldsymbol{x})$ through

$$\hat{y}(\mathbf{x}) = \sum_{i=1}^{n} \lambda_i \, \phi \left(||\mathbf{x} - \mathbf{x}_i|| \right) \quad (2)$$

where $\mathbf{x}$ is the vector of input variables, n is the number of sampling points, $\mathbf{x}_i$ is the vector of input variables at the ith sampling point, $\| \mathbf{x} - \mathbf{x}_i \| = \sqrt{(\mathbf{x} - \mathbf{x}_i)^T (\mathbf{x} - \mathbf{x}_i)}$ is the Euclidean norm representing the radial distance r from design point $\mathbf{x}$ to the sampling point $\mathbf{x}_i$, $\phi(.)$ is a radially symmetric basis function and λ_i are the unknown

interpolation coefficients. Commonly used RBF formulations include: $\phi(r) = r^2 \log(r)$ (thin-plate spline); $\phi(r) = e^{-\alpha r^2}$, $\alpha > 0$ (Gaussian); $\phi(r) = \sqrt{r^2 + c^2}$ (multiquadric); and $\phi(r) = 1/\sqrt{r^2 + c^2}$ (inverse multiquadric). In this study, multiquadric and inverse multiquadric formulations are considered. A suitable value of the parameter c in the multiquadrics approximation was recommended as $c = 1$ [58].

The unknown coefficients in Equation (2) are found by solving

$$[\mathbf{A}]\{\boldsymbol{\lambda}\} = \{\mathbf{y}\} \tag{3}$$

where $[\mathbf{A}] = \left[\phi \parallel \mathbf{x}_j - \mathbf{x}_i \parallel\right]$, $i,j = 1, \ldots, n$, $\{\boldsymbol{\lambda}\}^T = \{\lambda_1, \ldots, \lambda_n\}^T$ and $\{\mathbf{y}\}^T = \{y(x_1), \ldots, y(x_n)\}^T$.

3.3. Kriging, KR

Kriging metamodels estimate the true function $y(\boldsymbol{x})$ through

$$\hat{y}(x) = \mathbf{p}^{\mathrm{T}}(x)\boldsymbol{\beta} + Z(x) \tag{4}$$

The trend model $\mathbf{p}^{\mathrm{T}}(x)\boldsymbol{\beta}$ is a polynomial of given order (zeroth- and first-order models are often used) that globally approximates the response. The departure model $Z(x)$ is the stochastic component that generates deviations such that the Kriging model interpolates the sampled response data. The stochastic component has a mean value of zero and the following covariance

$$\mathrm{COV}[Z(\mathbf{x}^i), Z(\mathbf{x}^j)] = \sigma^2 \mathbf{R}[R(\mathbf{x}^i, \mathbf{x}^j)] \tag{5}$$

where $\mathbf{R}$ is an $n \times n$ correlation matrix if n is the number of training points, $R(\mathbf{x}^i, \mathbf{x}^j)$ is the correlation function between the two training points x^i and x^j. The most commonly used correlation function is the Gaussian function [28], which has the form of

$$R(\theta) = \prod_{k=1}^{N_v} \exp(-\theta_k d_k^2) \tag{6}$$

Once the correlation function has been estimated, the response is predicted as

$$\hat{y}(x) = \mathbf{p}^{\mathbf{T}}(x)\hat{\boldsymbol{\beta}} + \hat{\mathbf{r}}^{\mathbf{T}}(x)\hat{\mathbf{R}}^{-1}(\mathbf{F} - \mathbf{P}\hat{\boldsymbol{\beta}}) \tag{7}$$

where the vectors $\hat{\mathbf{r}}$ and $\hat{\boldsymbol{\beta}}$ are given by

$$\hat{\mathbf{r}}^T(x) = [\hat{R}(x, x^1), \hat{R}(x, x^2), \ldots, \hat{R}(x, x^n)]^T \tag{8.1}$$

$$\hat{\boldsymbol{\beta}} = (\mathbf{P}^{\mathbf{T}}\hat{\mathbf{R}}^{-1}\mathbf{P})^{-1}\mathbf{P}^{\mathbf{T}}\hat{\mathbf{R}}^{-1}\mathbf{F} \tag{8.2}$$

where $\hat{\mathbf{r}}^{\mathbf{T}}(x)$ is the correlation vector of length n between a prediction point x and the n sampling points, the $\hat{\mathbf{R}}$ matrix is obtained by using the predicted values $\hat{\theta}_k$ in Equation (6), $\mathbf{F}$ represents the responses at the n points and $\mathbf{P}$ is obtained by evaluating **p(x)** array at the n points.

The variance of Z in Equation (4) can be estimated as

$$\hat{\sigma}^2 = \frac{(\mathbf{F} - \mathbf{P}\hat{\boldsymbol{\beta}})^T \hat{\mathbf{R}}^{-1} (\mathbf{F} - \mathbf{P}\hat{\boldsymbol{\beta}})}{n} \tag{9}$$

The unknown model parameters θ_k can be estimated from [59]

$$\begin{aligned} \text{Max } \Phi(\boldsymbol{\Theta}) = & -[n \ln(\hat{\sigma}^2) + \ln|R|] \\ \text{s.t.} \quad & \boldsymbol{\Theta} > 0 \end{aligned} \tag{10}$$

where $|\mathbf{R}|$ is the determinant of $\mathbf{R}$, $\boldsymbol{\Theta}$ is the vector of unknown parameters θ_k, and both $\hat{\sigma}$ and $\mathbf{R}$ are functions of $\boldsymbol{\Theta}$. In this study, the MATLAB Kriging toolbox developed by Lophaven et al. [34] is used in the construction of Kriging metamodels.

4. Ensemble of metamodels

The most commonly followed practice in metamodelling studies is to construct many different types of metamodels and select the most accurate one while discarding the rest. There are two major drawbacks of this approach: (1) the efforts spent on constructing different metamodels are not fully utilised, (2) the performances of metamodels may depend on the training data set used, so the selected metamodel may not be the most accurate one for a different data set. One way to eliminate these shortcomings is to merge multiple metamodels into a weighted average ensemble of metamodel as in Equation (11)

$$\hat{y}_{\mathrm{ens}}(x) = \sum_{i=1}^{N_M} w_i \hat{y}_i(x) \tag{11}$$

where $\hat{y}_{\mathrm{ens}}$ is the response prediction obtained from the ensemble model, N_M is the number of metamodels in the ensemble, w_i is the contribution (or weight factor) of the ith metamodel in the ensemble and $\hat{y}_i$ is the response prediction obtained from the ith metamodel of the ensemble. To have an unbiased response estimation, the following equation must be satisfied by the weight factors:

$$\sum_{i=1}^{N_M} w_i = 1 \tag{12}$$

The weight factors in an ensemble are chosen such that an error metric is minimised. The error metric can be a global error metric [3,22,56,64] or a local error metric

[2,50]. In this paper, global error metrics are considered. The most popular global error metric used for selecting the weight factors in an ensemble is the mean square cross validation error (MSE_{cv}), which is computed as follows. If there are n training points, then a metamodel is constructed n times, each time leaving out one of the training points. Then, the difference between the exact response at the omitted point and the prediction response by each variant metamodel is used to evaluate the global error as

$$\text{MSE}_{\text{cv}} = \frac{1}{n}\sum_{k=1}^{n}(e^k)^2; e^k = y^k - \hat{y}^{(-k)} \tag{13}$$

where e^k is the cross validation error at the kth training point $\mathbf{x}^k$, y^k is the true response at $\mathbf{x}^k$ and $\hat{y}^{(-k)}$ is the corresponding predicted value from the metamodel constructed using all except the kth training point.

In this paper, the weight factor selection strategy proposed by Acar and Rais-Rohani [3] is used. Acar and Rais-Rohani [3] treated the selection of weight factors as an optimisation problem with the objective to minimise the MSE_{cv} of the ensemble model. That is, they computed the weight factors by solving

$$\text{Find } w_i, \;\; i = 1 \in N_M \tag{15.1}$$

$$\min \text{MSE}_{\text{cv}}\left\{\hat{y}_e\left(w_i, \hat{y}_i(x^k)\right), y(x^k), k = 1 \in n\right\} \tag{15.2}$$

$$\text{such that } \sum_{i=1}^{N_M} w_i = 1 \tag{15.3}$$

As MSE_{cv} is based on the difference between the exact response at the omitted training point and the predicted response by each variant metamodel at that point, this metric gives an average error at the training points. Even though it is often found that there is a strong positive correlation between MSE_{cv} and the actual mean squared error (MSE), depending on the behaviour of the response function as well as the number and distribution of training points (i.e., the geography of the design of experiments) MSE_{cv} may not necessarily provide a good resemblance of MSE. In this paper, two approaches are proposed to improve the correlation between MSE_{cv} and MSE as discussed in the next section.

5. Proposed approaches

To improve the correlation between MSE_{cv} and MSE and thereby increase the accuracy of response predictions, two approaches are proposed in this paper. The first approach is to remove outliers in the cross validation error set, and the second approach is to use an adjusted formulation for MSE_{cv}, where the outlier cross validation errors are down weighted.

The errors associated with the observations that are significantly different from the others, outliers, are often very large and have a greater influence on the mean square error than the smaller errors. Since MSE_{cv} is computed over a training set of limited number of points, outlier cross validation errors may have a substantial biased effect on MSE_{cv}. Therefore, an adjusted MSE_{cv} formulation based on outlier analysis may reduce the bias in MSE_{cv} and improve the correlation between MSE_{cv} and MSE.

There is no consensus in literature on what constitutes an outlier, and various methods have been proposed to detect outliers [26,48]. It is often assumed that the data are from a normal distribution, and the outliers are detected based on the mean and standard deviation of data. In this study, interquartile ranges are used to detect the outliers. That is, an observation outside the following range is considered to be an outlier

$$\text{IQR} = [Q_1 - k(Q_3 - Q_1), Q_1 + k(Q_3 - Q_1)] \tag{16}$$

where IQR is the interquartile range, Q_1 and Q_3 are the first and third quartiles, respectively, and k is a non-negative constant, for which a recommended value of 1.5 [55] is used in this study.

Once outliers are detected, they can be removed from data set or low weights can be assigned to the outliers [41]. In this paper, when the outlier cross validation errors are detected, two different approaches are followed to obtain an adjusted MSE_{cv} formulation: (1) the outlier cross validation errors are not used in MSE_{cv} calculation, (2) the outlier cross validation errors are down weighted in MSE_{cv} calculation based on their Mahalanobis distance. For the first adjustment, the adjusted MSE_{cv} formulation is obvious: the mean squared error is computed over the cross validation errors that are not outliers. For the second adjustment, the following formulation is used as an adjusted MSE_{cv} formula

$$(\text{MSE}_{\text{cv}})_{\text{adj}} = \frac{1}{n}\sum_{k=1}^{n}(e^k)^2_{\text{adj}} \tag{17.1}$$

$$(e^k)_{\text{adj}} = \begin{cases} e^k & \text{if } k \text{ is not outlier} \\ e^k \dfrac{(d_m^k)_{\text{ave}}}{d_m^k} & \text{if } k \text{ is outlier} \end{cases} \tag{17.2}$$

where d_m^k is the Mahalanobis distance of the cross validation error at kth training point, and $(d_m^k)_{\text{ave}}$ is the average value of the Mahalanobis distances of the cross validation errors that are not outliers.

6. Results and discussion

The first step of the metamodel construction is the determination of the training points in the input variable space

using a design of experiment technique. Latin hypercube sampling method is used in this study to generate 100 training points. Since two different crash scenarios (FFI and OFI) are considered, a total of 200 crash simulations are performed to compute the critical vehicle responses corresponding to training points. After the training set is formed, the metamodels are constructed (i.e., metamodel hyperparameters are determined) as discussed in Section 3. Then, the ensemble of metamodels is constructed (i.e., weight factors in the ensemble model are determined). Finally, the accuracy of metamodels (both individual and ensemble) is evaluated with an independent test set composed of 40 points. Since two different crash scenarios (FFI and OFI) are considered, a total of 80 crash simulations are performed to compute the critical vehicle responses corresponding to test points. Simulation results for the overall 280 crash simulations are provided in the appendix.

The accuracies of metamodels are measured with root mean square error evaluated at test points. To smooth the process of comparison of different models, the errors are normalised with respect to the most accurate individual metamodel among the five metamodels considered. Henceforth, the word 'normalised' is dropped when referring to the error.

The abbreviated symbols are used to identify the metamodels. For the individual metamodels, polynomial response surface is denoted by PRS, radial basis function with multiquadric and inverse multiquadric formulations are denoted by RBFm and RBFi, respectively, and Kriging models with zeroth- and first-order trend models are denoted by KR0 and KR1, respectively. For the ensemble models, the ensemble based on MSE_{cv} minimisation is labelled as ENS, and the ensemble based on adjusted MSE_{cv} minimisation is labelled as ENSa.

6.1. *Effect of removing the cross validation error outliers*

Table 2 shows the effect of removing the cross validation error outliers on the accuracy of ensemble of metamodels. The removal of the cross validation error outliers reduces the RMSE of the ensemble model on average by about 4.5%. The most effective RMSE reduction is achieved for the intrusion distance at the steering wheel for the FFI crash scenario, where the RMSE of the ensemble model is decreased by around 12%. Conversely, the least effective RMSE improvement (in fact, RMSE is increased in this case) is experienced for the intrusion distance at the steering wheel for the FFI crash scenario, where the RMSE of the ensemble model is increased by around 1%.

Table 2 also shows the accuracies of the individual metamodels. In general, RBF metamodels are the most accurate models for four out of six responses, whereas KR metamodels are the most accurate for the remaining two responses. The multiquadratic RBF model is found to be superior to the inverse multiquadratic RBF model. The performance of the KR1 model is found to be better than that of the KR0 model. The performance of the metamodels can also be compared with respect to the type of crash. RBF models are the most accurate for FFI, whereas KR models are the most accurate for OFI (except for the intrusion distance at steering wheel).

Figure 5 compares the boxplots of the cross validation errors with and without removal of the outlier errors for the FFI crash scenario. The boxplots provide a graphical depiction of how the cross validation errors vary over the range of training set. The bottom and top of each box represent the lower and upper quartile values, respectively, with the interior line representing the median. The broken line extending from each end of the box indicates 1.5 times

Table 2. Effect of removing outlier cross validation errors on the accuracy of ensemble of metamodels (metamodel accuracies are measured with normalised root mean square error evaluated at 40 test points).

Crash scenario	FFI			OFI		
Location of the intrusion distance	Floor panel	Driver seat	Steering wheel	Floor panel	Driver seat	Steering wheel
PRS	1.452	1.794	1.986	1.251	1.432	2.299
RBFm	1.010	1.000	1.000	1.103	1.148	1.000
RBFi	1.000	1.013	1.263	1.036	1.045	1.175
KR0	1.431	1.469	2.106	1.500	1.603	2.692
KR1	1.159	1.387	1.852	1.000	1.000	1.608
ENS	1.105	1.144	1.330	0.972	0.953	1.266
ENSa	1.041	1.058	1.345	0.944	0.951	1.119
Error ratio*	**0.942**	**0.925**	**1.011**	**0.971**	**0.998**	**0.884**

*The ratio of the RMSE of the ensemble based on MSE_{cv} to the RMSE of the ensemble based on adjusted MSE_{cv}. The average error ratio over the above six cases is 0.955.

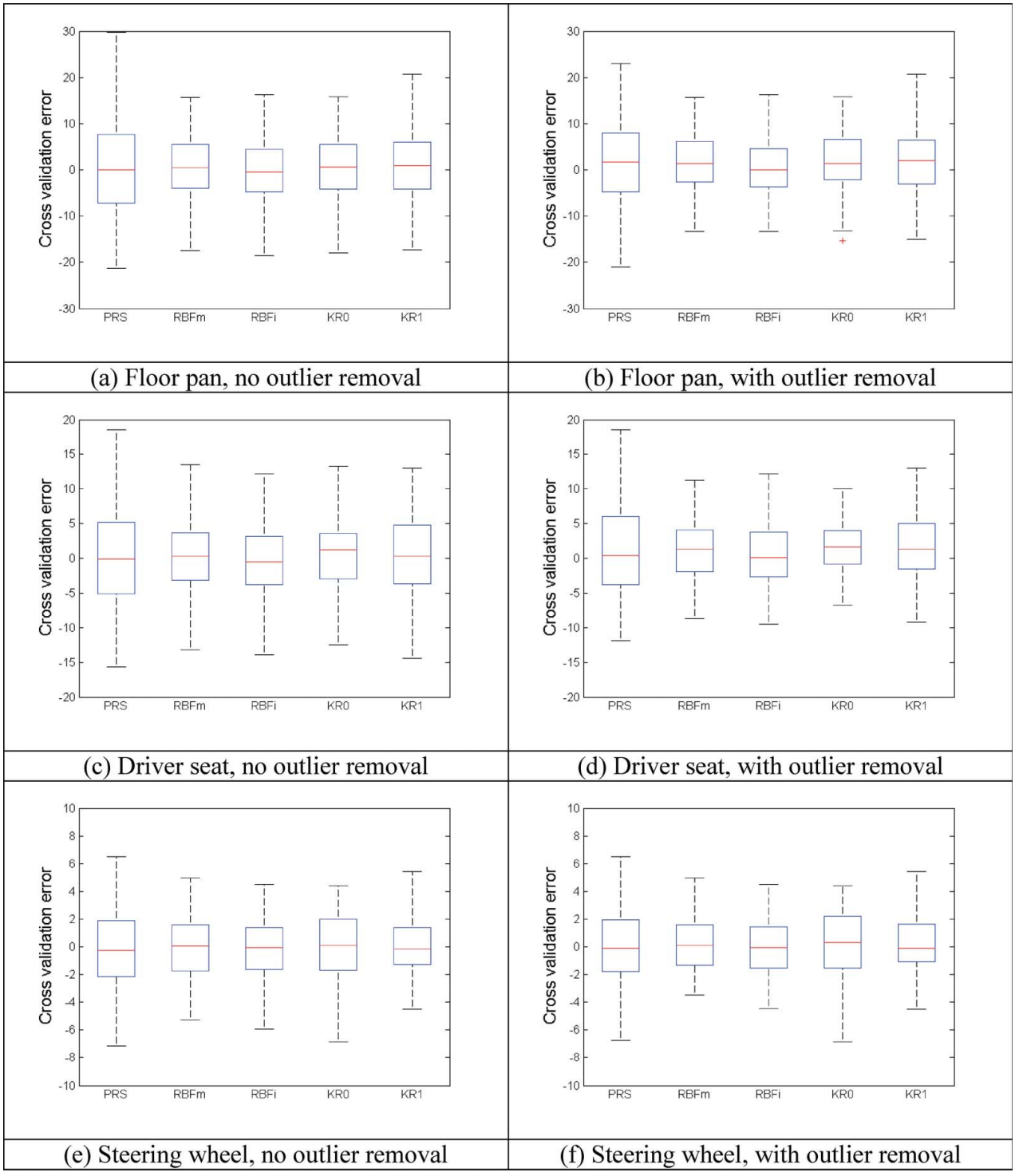

Figure 5. Boxplots of the cross validation errors for FFI crash scenario.

the interquartile range. Similarly, the comparison of the boxplots of the cross validation errors with and without removal of the outlier errors for the OFI crash scenario is depicted in Figure 6. It is observed in Figures 4 and 5 that the removal of the outlier errors reduces the scatter in cross validation error set, and this scatter reduction increases the correlation between the MSE and MSE_{cv} as explored in the next section.

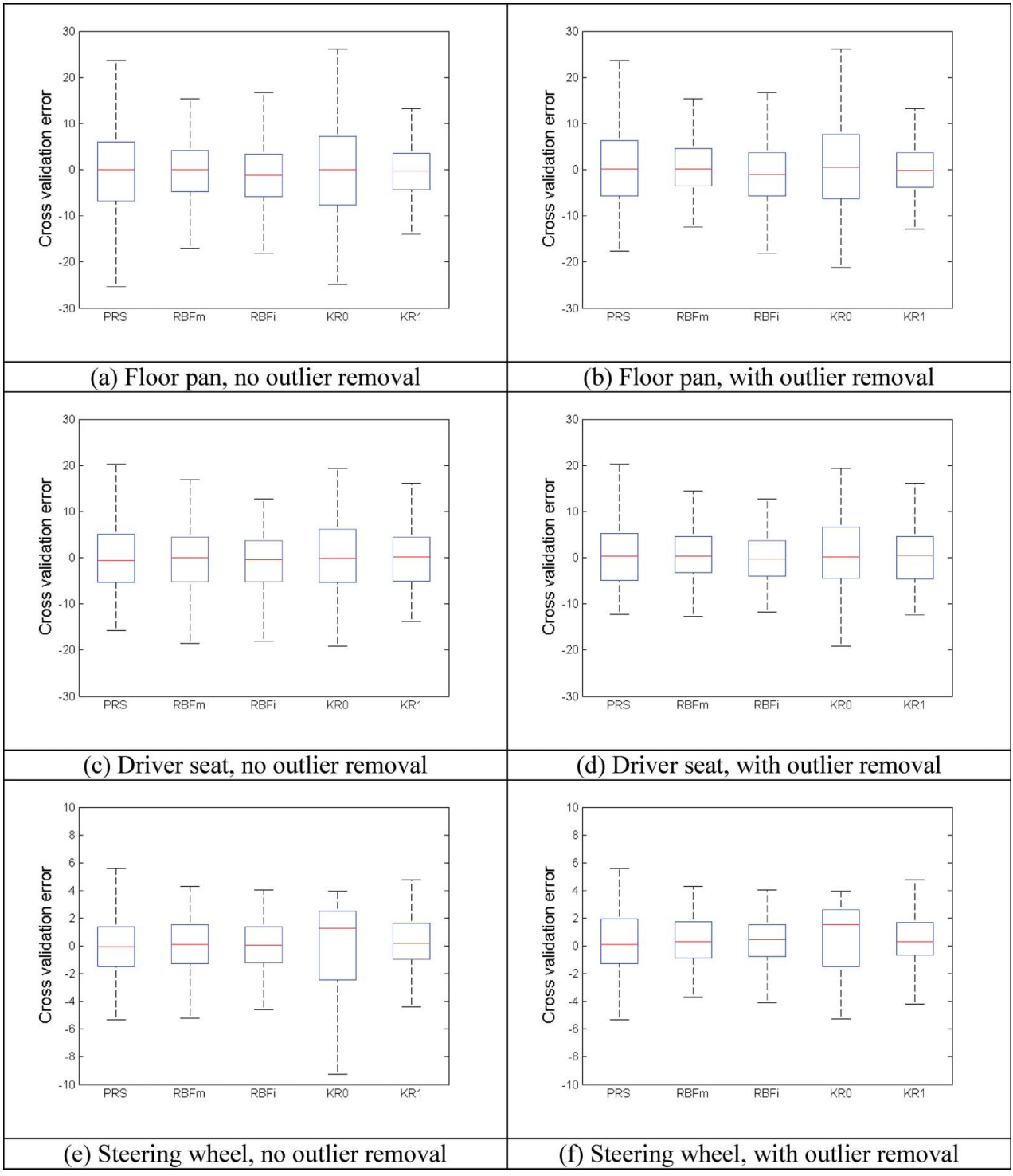

Figure 6. Boxplots of the cross validation errors for OFI crash scenario.

6.2. *Correlation between the cross validation error and actual error*

The effect of the removal of the outlier cross validation errors on the correlation between the cross validation error and actual error is explored in this section. Table 3 shows the root mean square cross validation errors evaluated at training points ($RMSE_{cv}$) and root mean square errors evaluated at the test points (RMSE) for the ensemble of metamodels. The correlation coefficient between $RMSE_{cv}$ and RMSE is computed over the six critical crash

Table 3. Root mean square cross validation errors ($RMSE_{cv}$) and root mean square errors evaluated at test points (RMSE) for the ensemble of metamodels.

Crash scenario	FFI			OFI		
Location of the intrusion distance	Floor panel	Driver seat	Steering wheel	Floor panel	Driver seat	Steering wheel
$RMSE_{cv}$						
ENS	7.491	6.149	2.159	7.909	6.993	2.129
ENSa	7.628	6.191	2.164	7.993	7.093	2.173
RMSE						
ENS	5.169	3.901	1.425	4.734	3.969	1.376
ENSa	4.868	3.609	1.441	4.597	3.961	1.216

responses. It is found that the removal of outlier cross validation errors increases the correlation coefficient from 0.983 to 0.991. This improvement leads to a better choice of weight factors of individual metamodels in the ensemble and reduces the RMSE of the ensemble models as shown in the previous section.

To compute the correlation coefficient between $RMSE_{cv}$ and RMSE, two arrays are generated first. For the original ensemble, for instance, the first array is composed of $RMSE_{cv}$ values in the first row of Table 3, that is, $\mathbf{A_1} = \{7.491, 6.149, 2.159, 7.909, 6.993, 2.129\}$. The second array is composed of the RMSE values in the third row of Table 3, that is, $\mathbf{A_2} = \{5.169, 3.901, 1.425, 4.734, 3.969, 1.376\}$. Then, the correlation coefficient between the arrays $\mathbf{A_1}$ and $\mathbf{A_2}$ is computed to be 0.983 from the following equation:

$$\rho = \frac{C_{12}}{\sqrt{C_{11}C_{22}}} \tag{18}$$

where C_{ij} denotes the element in row i and column j of matrix $\mathbf{C}$, which is the covariance matrix of $\mathbf{A}$. Matrix $\mathbf{A}$ is formed with arrays $\mathbf{A_1}$ and $\mathbf{A_2}$ as $\mathbf{A} = [\mathbf{A_1}^T, \mathbf{A_2}^T]$. Similarly, the errors in the second and fourth rows of Table 3 are used to calculate the correlation coefficient between $RMSE_{cv}$ and RMSE for the ensemble based on removal of outlier cross validation errors.

6.3. *Effect of weighting down the outlier cross validation errors*

Alternative to removing the outlier cross validation errors in MSE_{cv} calculation is to use an adjusted formula for MSE_{cv} calculation where smaller weights are used for the outliers (see Equation (17)). Table 4 shows the effect of weighing down the outlier cross validation errors on the accuracy of ensemble of metamodels. It is found that this practice yields results very close to those of outlier error removal. The RMSE of the ensemble model is reduced on average by about 4.4%.

7. Conclusions

Metamodels that can mimic the behaviour of the crash simulation models emerge as a solution to the computational burden on simulation based optimisation studies.

Table 4. Effect of weighting down outlier cross validation errors on the accuracy of ensemble of metamodels (metamodel accuracies are measured with normalised root mean square error evaluated at 40 test points).

Crash scenario	FFI			OFI		
Location of the intrusion distance	Floor panel	Driver seat	Steering wheel	Floor panel	Driver seat	Steering wheel
PRS	1.452	1.794	1.986	1.251	1.432	2.299
RBFm	1.010	1.000	1.000	1.103	1.148	1.000
RBFi	1.000	1.013	1.263	1.036	1.045	1.175
KR0	1.431	1.469	2.106	1.500	1.603	2.692
KR1	1.159	1.387	1.852	1.000	1.000	1.608
ENS	1.105	1.144	1.330	0.972	0.953	1.266
ENSa	1.042	1.060	1.347	0.944	0.952	1.118
Error ratio*	**0.942**	**0.927**	**1.013**	**0.971**	**0.999**	**0.883**

*The ratio of the RMSE of the ensemble based on MSE_{cv} to the RMSE of the ensemble based on adjusted MSE_{cv}. The average error ratio over the above six cases is 0.956.

Prediction capability in metamodelling can be improved by combining many different metamodels in the form of an ensemble model. In this paper, two approaches based on outlier analysis of cross validation errors were proposed to increase the accuracy of ensemble models constructed for crash response predictions. Full frontal and offset frontal crash response predictions of a c-class passenger car were used for demonstration. The first approach was to remove outliers in the cross validation error set, and the second approach was to weigh down the outliers in the cross validation error set. From the results obtained in this study, the following conclusions could be drawn:

- The most effective error reduction is achieved for the intrusion distance at the steering wheel for the full frontal crash scenario, where the ensemble model error is decreased by around 12%.
- Conversely, the least effective error reduction (in fact, error is increased in this case) was experienced for the intrusion distance at the steering wheel for the offset frontal crash scenario, where the RMSE of the ensemble model is increased by around 1%.
- The removal of the cross validation error outliers reduces the error of the ensemble model on average by about 4.5%.
- RBF metamodels, in general, were the most accurate for response prediction of FFI, whereas Kriging models were the most accurate for response prediction of OFI.
- Removal of outlier cross validation errors increased the correlation coefficient between the cross validation error and the actual error from 0.983 to 0.991.
- Alternative to removing the outlier cross validation errors, the effect of weighing down the outlier cross validation errors was explored. It was found that this practice yields results very close to those of outlier error removal.

In this study, it is assumed that the crash simulation results are robust. That is, it is assumed that repeating the crash simulations using a parallel computation scheme does not lead to significantly different results. However, this might not be the case. It is well known that some physical and/or numerical instabilities might be observed in some of the crash simulations (for instance, due to deformation bifurcation of side rails). Therefore, there might be a strong positive correlation between the cross validation error outliers and non-robust crash simulations. Investigation of the correlation between the outliers and non-robust crash simulations is beyond the scope of this paper and planned to be addressed in a future study.

Acknowledgements

The author wishes to thank Dr. Kiran Solanki for performing the crash simulations.

References

[1] E. Acar, *Optimising shape parameters of radial basis functions: An application to automobile crashworthiness*, Proc. Institution Mech. Eng. D: J. Automobile Eng. 224(12) (2010), pp. 1541–1553.

[2] E. Acar, *Various approaches for constructing an ensemble of metamodels using local measures*, Struct. Multidiscip. Optim. 42(6) (2010), pp. 879–896.

[3] E. Acar and M. Rais-Rohani, *Ensemble of metamodels with optimized weight factors*, Struct. Multidiscip. Optim. 37(3) (2009), pp. 279–294.

[4] E. Acar and K. Solanki, *Improving the accuracy of vehicle crashworthiness response predictions using an ensemble of metamodels*, Int. J. Crashworthiness 14 (2009), pp. 49–61.

[5] Anonymous, *NHTSA vehicle safety and fuel economy rulemaking and research priority plan 2011-2013*, 2011. Available at http://www.nhtsa.gov/staticfiles/rulemaking/pdf/2011-2013_Vehicle_Safety-Fuel_Economy_Rulemaking-Research_Priority_Plan.pdf.

[6] Anonymous, *2012 motor vehicle crashes: Overview*. NHTSA traffic safety facts, DOT HS 811 856, 2013. Available at www-nrd.nhtsa.dot.gov/Pubs/811856.pdf.

[7] C. Baykasoglu, E. Sunbuloglu, S.E. Bozdag, F. Aruk, T. Toprak, and A. Muga, *Crash and structural analyses of an aluminium railroad passenger car*, Int. J. Crashworthiness 17(5) (2012), pp. 519–528.

[8] C.M. Bishop, *Neural Networks for Pattern Recognition*, Oxford University Press Inc., New York, 1995.

[9] G.E.P. Box, W.G. Hunter, and J.S. Hunter, *Statistics for Experimenters*, John Wiley & Sons, New York, 1978.

[10] M.D. Buhmann, *Radial Basis Functions: Theory and Implementations*, Cambridge University Press, New York, 2003.

[11] L. Cheah, C. Evans, A. Bandivadekar, and J. Heywood, Factor of two: Halving the fuel consumption of new U.S. automobiles by 2035, in *Reducing Climate Impacts in the Transportation Sector*, J.S. Cannon and D. Sperling, eds., Springer, Netherlands, 2009, pp. 49–71.

[12] S.M. Clarke, J.H. Griebsch, and T.W. Simpson, *Analysis of support vector regression for approximation of complex engineering analyses*, J. Mech. Des. 127(11) (2005), pp. 1077–1087.

[13] K.J. Craig, N. Stander, D.A. Dooge, and S. Varadappa, *Automotive crashworthiness design using response surface based variable screening and optimization*, Eng. Comput. 22(1) (2005), pp. 38–61.

[14] N. Cristello and I.L. Kim, *Multidisciplinary design optimization of a zero-emission vehicle chassis considering crashworthiness and hydroformability*, Proc. Institution Mech. Eng. D: J. Automobile Eng. 221(5) (2007), pp. 511–526.

[15] J. Davis, *The potential for vehicle weight reduction using magnesium*, SAE Tech. Paper 910551, Society of Automotive Engineers Inc., Warrendale, 1991. DOI:10.4271/910551.

[16] N. Dyn, D. Levin, and S. Rippa, *Numerical procedures for surface fitting of scattered data by radial basis functions*, SIAM J. Sci. Stat. Comput. 7(2) (1986), pp. 639–659.

[17] H. Fang, M. Rais-Rohani, Z. Liu, and M.F. Horstemeyer, *A comparative study of metamodeling methods for multiobjective crashworthiness optimization*, Comput. Struct. 83 (25−26) (2005), pp. 2121−2136.

[18] H. Fang, K. Solanki, and M. Horstemeyer, *Energy-based crashworthiness optimization for multiple vehicle impacts*, International Mechanical Engineering Congress and Exposition, Transportation: Transportation and Environment, November 13−19, Anaheim, CA, 2004, Paper No. IMECE2004-59123.

[19] H. Fang, K. Solanki, and M. Horstemeyer, *Numerical simulations of multiple vehicle crashes and multidisciplinary crashworthiness optimization*, Int. J. Crashworthiness 10 (2) (2005), pp. 161−172.

[20] P. Feng, *Ensemble of surrogate models for lightweight design of autobody structure*, Ph.D. thesis, Shanghai Jiaotong University, Shanghai, China, 2011.

[21] J. Forsberg and L. Nilsson, *On polynomial response surfaces and Kriging for use in structural optimization of crashworthiness*, Struct. Multidiscip. Optim. 29(3) (2005), pp. 232−243.

[22] T. Goel, R.T. Haftka, W. Shyy, and N.V. Queipo, *Ensemble of surrogates*, Struct. Multidiscip. Optim. 33(3) (2007), pp. 199−216.

[23] L. Gu, *A comparison of polynomial based regression models in vehicle safety analysis*, ASME Design Engineering Technical Conferences, Pittsburgh, PA, 2001, Paper No. DETC2001/DAC-21063.

[24] S.R. Gunn, *Support vector machines for classification and regression*, Tech. Rep., Image Speech and Intelligent Systems Research Group, University of Southampton, Southampton, UK, 1997.

[25] K. Hamza and K. Saitou, *Crashworthiness design using meta-models for approximating the response of structural members*, Proceeding of MDP-8, Cairo University Conference on Mechanical Design and Production, Cairo, Egypt, 2004, pp. 591−601.

[26] V.J. Hodge and J. Austin, *A survey of outlier detection methodologies*, Artif. Intell. Rev. 22 (2004), pp. 85−126.

[27] H. Ibrahim, *Material optimization for design improvement of crash energy absorbers*, Proc. ASME Int. Mech. Eng. Congress Exposition 11 (2010), pp. 653−663.

[28] R. Jin, W. Chen, and T.W. Simpson, *Comparative studies of metamodelling techniques under multiple modelling criteria*, Struct. Multidiscip. Optim. 23(1) (2001), pp. 1−13.

[29] M. Kiani, I. Gandikota, A. Parrish, K. Motoyama, and M. Rais-Rohani, *Surrogate-based optimisation of automotive structures under multiple crash and vibration design criteria*, Int. J. Crashworthiness 18(5) (2013), pp. 473−482.

[30] M. Kiani, K. Motoyama, M. Rais-Rohani, and H. Shiozaki, *Joint stiffness analysis and optimization as a mechanism for improving the structural design and performance of a vehicle*, Proc. Institution Mech. Eng. D: J. Automobile Eng. 228(6) (2014), pp. 689−700.

[31] Y. Kurihara, *The role of aluminum in automotive weight reduction*, J. Minerals Metals Mater. Soc. 45(11) (1993), pp. 32−33.

[32] D.C. Lee and J.I. Lee, *A structural optimization design for an aluminum-intensive vehicle*, Proc. Institution Mech. Eng. D: J. Automobile Eng. 217(9) (2003), pp. 771−779.

[33] T.H. Lee and J.M. Lee, *Full frontal crashworthiness design optimization of a vehicle using the statistical space-time Kriging metamodel based on multiple responses approach*, 9th World Congress on Structural and Multidisciplinary Optimization, June 13−17, Shizuoka, Japan, 2011.

[34] S.N. Lophaven, H.B. Nielsen, and J. Søndergaard, *DACE − a MATLAB Kriging toolbox*, Informatics and Mathematical Modeling, Technical University of Denmark, Lyngby, Denmark, 2002.

[35] R. Lust, *Structural optimization with crashworthiness constraints*, Struct. Multidiscip. Optim. 4 (1992), pp. 85−89.

[36] D.J.C. MacKay, *Introduction to Gaussian processes*, in *Neural Networks and Machine Learning*, Vol. 168 of NATO ASI Series, C.M. Bishop, ed., Springer, Berlin, 1998, pp. 133−165.

[37] R.H. Myers and D.C. Montgomery, *Response Surface Methodology: Process and Product Optimization Using Designed Experiments*, Wiley, New York, 2002.

[38] T. Omar, A. Eskandarian, and N. Bedewi, *Vehicle crash modelling using recurrent neural networks*, Math. Comput. Model. 28 (1998), pp. 31−42.

[39] F. Pan and P. Zhu, *Design optimisation of vehicle roof structures: Benefits of using multiple surrogates*, Int. J. Crashworthiness 16(1) (2011), pp. 85−95.

[40] F. Pan, P. Zhu, and Y. Zhang, *Metamodel-based lightweight design of B-pillar with TWB structure via support vector regression*, Comput. Struct. 88(1−2) (2010), pp. 36−44.

[41] M Papila and R.T. Haftka, *Response surface approximations: Noise, error repair, and modeling errors*, AIAA J. 38(12) (2000), pp. 2336−2343.

[42] A. Parrish, M. Rais-Rohani, and A. Najafi, *Crashworthiness optimisation of vehicle structures with magnesium alloy parts*, Int. J. Crashworthiness 17(3) (2012), pp. 259−281.

[43] Partnership of a New Generation of Vehicles, ULSA-BAVC Program, May 1999. Available at http://www.corusautomotive.com/file_source/automotive/Publications/ULSAB-TTD1.pdf.

[44] L. Patberg, M. Philipps, and R. Dittmann, *Fibre-reinforced composites in the car side structure*, Proc. Institution Mech. Eng. D: J. Automobile Eng. 213(5) (1999), pp. 417−423.

[45] C. Qi and S. Yang, *Crashworthiness and lightweight optimisation of thin-walled conical tubes subjected to an oblique impact*, Int. J. Crashworthiness 19(4) (2014), pp. 334−351.

[46] N.V. Queipo, R.T. Haftka, W. Shyy, T. Goel, R. Vaidyanathan, and P.K. Tucker, *Surrogate-based analysis and optimization*, Prog. Aerosp. Sci. 41 (2005), pp. 1−28.

[47] C.E. Rasmussen and C.K.I. Williams, *Gaussian Processes for Machine Learning*, MIT Press, Cambridge, MA, 2006.

[48] P. Rousseeuw and A. Leroy, *Robust Regression and Outlier Detection*, 3rd ed., John Wiley & Sons, New York, NY, 1996.

[49] J. Sacks, W.J. Welch, T.J. Mitchell, and H.P. Wynn, *Design and analysis of computer experiments*, Stat. Sci. 4 (4) (1989), pp. 409−435.

[50] E. Sanchez, S. Pintos, N.V. Queipo, *Toward an optimal ensemble of kernel-based approximations with engineering applications*, Struct. Multidiscip. Optim. 36(3) (2008), pp. 247−261.

[51] T.W. Simpson, T.M. Mauery, J.J. Korte, and F. Mistree, *Kriging models for global approximation in simulation-based multidisciplinary design optimization*, AIAA J. 39 (12) (2001), pp. 2233−2241.

[52] M. Smith, *Neural Networks for Statistical Modeling*, Van Nostrand Reinhold, New York, 1993.

[53] N. Stander, W. Roux, M. Giger, M. Redhe, N. Fedorova, and J. Haarhoff, *A comparison of metamodeling techniques for crashworthiness optimization*, 10th AIAA/ISSMO Multidisciplinary Analysis and Optimization Conference, Albany, NY, 2004, AIAA Paper No. 2004-4489.

[54] N. Tavassoli, B. Notghi, A. Darvizeh, and M. Darvizeh, *Multi-objective crashworthiness optimization of composite*

hat-shape energy absorber using GMDH-type neural networks and genetic algorithms, International Mechanical Engineering Congress and Exposition, Volume 3: Design and Manufacturing, Parts A and B, November 12–18, Vancouver, British Columbia, Canada, 2010, Paper No. IMECE2010-38693.

[55] J.W. Tukey, *Exploratory Data Analysis*, Addison-Wesley, Reading, MA, 1977.

[56] F.A.C. Viana, R.T. Haftka, and V. Steffen, *Multiple surrogates: How cross-validation errors can help us to obtain the best predictor*, Struct. Multidiscip. Optim. 39(6) (2009), pp. 439–457.

[57] H. Wallentowitz and H. Adam, *Predicting the crashworthiness of vehicle structures made by lightweight design materials and innovative joining methods*, Int. J. Crashworthiness 1(2) (1996), pp. 163–180.

[58] L. Wang, D. Beeson, G. Wiggs, and M. Rayasam, *A comparison of metamodeling methods using practical industry requirements*, Proceedings of the 47th AIAA/ASME/ASCE/AHS/ASC Structures, Structural Dynamics, and Materials Conference, Newport, RI, 2006.

[59] G.G. Wang and S. Shan, *Review of metamodeling techniques in support of engineering design optimization*, J. Mech. Des. 129(4) (2007), pp. 370–380.

[60] R.J. Yang, N. Wang, C.H. Tho, J.P. Bobineau, and B.P. Wang, *Metamodeling development for vehicle frontal impact simulation*, J. Mech. Des. 127(5) (2005), pp. 1014–1020.

[61] A.R. Yildiz and K. Saitou, *Topology synthesis of multicomponent structural assemblies in continuum domains*, J. Mech. Des. 133(1) (2011), pp. 011008–1–011008-9.

[62] A.R. Yildiz and K. Solanki, *Multi-objective optimization of vehicle crashworthiness using a new particle swarm based approach*, Int. J. Adv. Manuf. Technol. 59 (2012), pp. 367–376.

[63] H. Yin, G. Wen, H. Fang, Q. Qing, X. Kong, J. Xiao, and Z. Liu, *Multiobjective crashworthiness optimization design of functionally graded foam-filled tapered tube based on dynamic ensemble metamodel*, Mater. Des. 55 (2014), pp. 747–757.

[64] X.J. Zhou, Y.Z. Ma, Y.L. Tub, and Y. Feng, *Ensemble of surrogates for dual response surface modeling in robust parameter design*, Qual. Reliab. Eng. Int. 29(2) (2012), pp. 173–197.

Appendix. Crash simulation results

Training points, test points and corresponding responses (intrusion distances) used in metamodel construction and accuracy evaluation for FFI and OFI crash scenarios are provided in Table A1 and A2.

Table A1. Training points and corresponding responses (intrusion distances) for both crash scenarios.

	Input variables									FFI responses (mm)			OFI responses (mm)		
ID #	x1	x2	x3	x4	x5	x6	x7	x8	x9	FP	DS	SW	FP	DS	SW
1	0.179	0.098	0.008	0.184	1.038	−7.576	35.76	16.17	128.9	52.89	37.31	12.80	63.01	46.61	7.96
2	0.174	−0.129	0.104	0.008	0.770	−2.525	28.48	14.60	129.8	50.68	31.29	13.84	54.59	35.11	14.92
3	−0.003	0.058	−0.038	−0.225	1.028	2.525	41.41	15.83	57.3	59.49	41.51	8.16	69.21	55.11	6.31
4	−0.184	−0.124	0.149	0.098	1.078	5.556	45.05	16.13	123.4	52.12	33.29	9.91	60.43	36.64	8.01
5	0.194	−0.210	−0.230	−0.058	1.215	3.737	37.37	15.24	132.5	64.39	24.83	11.69	52.97	41.06	5.78
6	0.230	0.068	0.174	−0.008	1.104	−4.545	32.53	15.38	127.9	51.52	37.31	9.23	56.64	42.83	7.45
7	−0.093	−0.189	−0.159	0.053	0.947	5.960	43.03	14.62	50.0	54.66	37.90	8.11	73.89	54.86	6.83
8	0.154	−0.174	−0.220	0.048	1.179	9.798	53.94	14.88	80.3	52.26	37.18	9.60	76.11	52.56	5.73
9	−0.114	0.225	−0.245	0.013	1.003	8.586	30.10	16.66	61.0	59.21	38.28	10.57	58.97	38.55	8.92
10	−0.063	−0.240	−0.225	0.114	0.967	6.162	50.71	15.43	126.1	60.52	44.10	9.15	69.39	45.98	5.37
11	−0.205	−0.230	0.073	0.119	1.199	−4.747	49.09	14.79	81.2	75.16	48.56	11.80	79.78	54.30	5.03
12	−0.048	−0.235	−0.169	−0.169	0.886	4.949	43.43	14.94	75.7	69.17	49.11	9.73	74.18	51.83	6.89
13	0.038	0.189	−0.053	0.129	0.851	−7.778	47.88	14.75	120.6	57.64	37.14	12.37	64.01	41.28	9.35
14	−0.179	0.053	0.225	−0.215	1.053	−3.939	39.39	15.32	86.7	53.00	26.30	14.89	66.20	39.79	9.44
15	0.164	−0.078	0.043	0.210	0.811	8.788	39.80	16.38	114.2	55.97	41.11	13.91	63.65	49.73	8.17
16	0.129	0.240	−0.063	−0.220	1.139	−2.929	48.69	15.89	110.5	57.31	39.43	9.08	68.98	46.34	7.64
17	0.098	0.104	−0.018	0.159	0.992	−2.121	40.20	16.04	92.2	60.97	42.05	12.24	69.20	50.15	6.37
18	−0.023	0.164	0.235	−0.048	1.220	6.768	22.42	15.41	74.7	53.04	32.46	14.25	47.67	28.84	11.10
19	0.199	−0.139	0.053	−0.053	0.912	0.101	53.54	16.36	82.1	53.50	32.36	8.32	79.58	53.03	5.08
20	0.124	0.018	−0.210	0.230	1.114	2.323	23.23	15.96	58.2	62.78	40.94	10.94	51.70	31.65	16.21
21	0.013	−0.215	0.169	0.028	0.977	−9.596	42.63	15.19	97.7	77.58	54.06	11.91	72.43	49.86	7.26
22	0.053	0.033	0.078	0.134	1.109	−2.727	24.44	15.55	131.6	56.75	40.40	8.54	46.84	32.89	15.35
23	−0.154	−0.109	0.063	0.164	0.896	0.909	22.83	16.45	83.9	69.55	42.72	17.48	58.50	39.73	11.23

(*continued*)

Table A1. (*Continued*)

	Input variables									FFI responses (mm)			OFI responses (mm)		
ID #	x1	x2	x3	x4	x5	x6	x7	x8	x9	FP	DS	SW	FP	DS	SW
24	−0.124	−0.018	−0.058	−0.245	0.846	9.394	36.57	15.53	90.3	70.93	49.79	13.46	76.52	56.46	6.31
25	0.078	−0.179	0.230	−0.038	0.790	−3.535	46.67	16.15	62.8	85.20	59.13	9.22	78.45	45.92	6.55
26	0.018	0.003	0.144	−0.199	0.891	6.364	51.92	15.98	127.0	69.38	51.32	11.44	86.05	60.41	6.94
27	−0.043	−0.245	−0.109	−0.164	1.184	−6.566	22.02	15.68	88.5	52.24	34.61	13.80	43.46	26.61	15.06
28	0.149	−0.058	−0.078	0.139	1.144	−6.364	27.27	16.62	122.4	55.23	38.60	10.70	47.84	33.14	12.05
29	0.225	0.109	−0.068	−0.124	1.159	−6.162	45.86	16.34	107.8	47.53	34.74	10.11	71.45	56.85	7.01
30	−0.240	0.023	−0.119	−0.179	1.134	−9.192	55.96	15.62	108.7	43.01	30.37	7.48	69.86	52.93	13.40
31	0.114	−0.083	0.048	−0.205	0.821	−3.333	55.15	16.25	49.1	65.44	45.94	9.59	88.28	54.15	6.49
32	0.169	−0.073	−0.083	0.144	0.801	−0.505	49.90	16.23	60.1	66.68	46.55	11.01	85.52	64.99	6.84
33	0.189	−0.250	−0.023	−0.230	0.795	−6.768	50.30	15.85	94.0	55.57	33.89	7.83	69.32	46.86	6.96
34	0.073	−0.194	0.154	−0.149	0.841	−4.343	56.36	16.64	106.9	59.57	41.65	12.01	79.77	49.20	7.65
35	0.139	0.199	−0.093	−0.235	0.856	−4.949	34.95	16.00	136.2	48.99	28.24	19.59	59.73	42.08	8.41
36	−0.225	0.129	−0.104	0.154	1.129	−6.970	38.59	16.59	68.3	53.89	33.75	13.45	63.60	45.14	6.14
37	−0.194	0.144	0.189	0.003	1.093	1.111	26.06	15.81	119.7	50.52	28.40	16.23	50.02	28.16	11.80
38	0.063	0.088	−0.164	0.205	1.063	4.141	33.74	16.11	111.4	62.41	42.69	8.17	62.15	46.69	5.64
39	0.008	0.134	0.194	0.083	0.816	3.535	57.17	15.64	105.0	55.01	38.64	10.47	70.03	44.19	6.99
40	−0.174	−0.114	−0.088	0.240	0.962	−8.384	52.32	15.92	83.0	78.95	56.94	7.56	92.58	64.61	6.19
41	0.240	0.008	0.205	0.189	0.775	3.333	60.00	16.47	72.0	59.16	41.63	7.49	86.97	65.67	8.00
42	−0.028	−0.063	−0.205	−0.134	0.982	5.152	31.31	14.77	67.4	67.85	44.81	7.68	60.59	42.33	8.40
43	0.048	0.220	−0.048	0.093	0.866	−5.152	57.58	16.40	56.4	60.87	42.21	9.34	80.74	51.69	6.18
44	−0.144	0.230	0.013	−0.189	0.952	−3.737	47.47	14.96	101.3	57.85	37.93	11.53	73.51	45.76	6.87
45	0.144	−0.169	0.003	−0.139	1.245	−0.303	48.28	14.92	52.7	59.92	43.85	9.69	78.19	58.43	8.12
46	−0.134	−0.164	0.245	0.194	0.765	−1.313	43.84	15.17	77.5	56.46	34.30	12.63	76.84	46.37	8.12
47	−0.058	0.124	−0.028	−0.003	1.008	8.384	44.24	14.73	91.3	53.66	35.61	9.57	67.59	49.67	6.35
48	0.205	−0.104	0.164	−0.184	1.189	−1.919	28.89	16.08	98.6	44.95	29.77	12.66	47.55	33.97	11.50
49	−0.104	0.159	0.134	0.088	0.937	2.727	31.72	14.71	66.5	65.41	39.10	15.16	69.14	44.72	11.53
50	−0.210	0.235	0.058	0.225	0.780	−8.586	20.81	15.77	85.8	58.36	34.22	16.28	63.90	38.57	17.51
51	−0.129	−0.159	0.250	−0.250	1.250	8.182	53.13	15.47	94.9	63.37	45.27	9.31	85.44	62.94	9.18
52	−0.245	0.038	−0.003	−0.114	0.902	3.939	24.04	15.26	79.3	60.79	35.34	12.80	64.08	41.13	15.47
53	0.210	0.043	0.220	0.043	1.023	1.717	26.46	15.09	130.7	45.47	32.86	12.49	47.53	34.63	11.59
54	0.083	−0.008	0.114	−0.023	1.043	1.919	29.29	15.30	102.3	57.69	39.49	9.26	57.31	41.17	10.83
55	−0.109	−0.048	0.184	−0.078	0.760	10.000	51.52	14.81	48.2	88.66	60.40	7.74	82.96	49.13	6.58
56	−0.250	−0.199	−0.184	0.038	1.033	−2.323	30.91	16.57	124.3	51.68	33.42	11.56	59.57	49.79	10.34
57	−0.235	0.149	−0.144	0.124	1.164	−10.000	58.38	15.66	121.5	42.21	31.86	9.86	70.10	53.07	7.64
58	−0.119	−0.033	0.139	0.245	0.861	−8.182	35.35	16.06	55.5	78.50	51.16	15.39	78.49	51.42	10.86
59	−0.053	0.119	−0.215	0.174	0.881	−3.131	27.68	15.36	99.5	61.17	39.99	12.60	53.76	34.34	14.17
60	−0.220	0.245	0.240	0.033	1.119	1.313	32.93	16.53	84.8	55.90	34.31	15.32	64.45	42.28	11.92
61	0.245	0.073	0.159	0.078	0.997	5.354	41.01	16.68	78.4	47.78	34.16	7.48	61.71	45.96	6.22
62	0.068	−0.220	−0.189	−0.033	0.907	−7.980	51.11	16.02	76.6	64.84	45.39	7.70	30.03	24.50	7.17
63	0.220	0.205	0.023	−0.109	0.755	3.131	26.87	16.42	63.7	65.25	41.33	11.58	65.25	41.33	11.58
64	0.023	−0.028	−0.073	0.250	1.225	5.758	34.14	15.22	103.2	66.15	48.50	11.02	57.20	44.02	7.40
65	−0.008	−0.119	−0.114	−0.174	1.058	−0.707	46.26	16.30	59.2	63.59	44.19	9.50	75.48	56.44	6.34
66	−0.169	0.210	0.093	0.109	0.831	−4.141	57.98	16.32	116.0	49.28	34.28	12.52	76.43	44.77	6.00
67	−0.018	−0.003	−0.235	−0.083	1.088	7.980	54.34	15.75	50.9	75.76	54.96	12.07	89.44	67.57	12.56
68	−0.230	−0.205	0.199	0.073	1.205	−1.111	20.00	15.60	61.9	62.47	34.85	18.46	58.05	31.41	18.11
69	0.134	0.174	0.068	0.063	1.210	6.566	38.99	16.55	100.4	57.03	44.09	11.52	65.13	48.10	8.01
70	−0.189	0.028	−0.124	0.104	1.194	−8.788	54.75	15.11	113.3	43.16	32.60	9.24	76.16	56.69	10.71
71	−0.068	0.179	0.129	−0.154	1.068	−5.960	36.16	15.05	45.4	73.49	46.68	8.83	81.50	56.90	5.31
72	0.159	0.114	0.215	0.068	0.942	−7.172	42.22	16.49	134.4	49.90	33.10	13.26	74.52	53.29	5.33
73	−0.073	0.093	0.179	−0.088	1.169	2.929	24.85	16.28	46.3	64.18	37.16	15.29	63.55	40.47	10.98

(*continued*)

Table A1. (*Continued*)

	Input variables									FFI responses (mm)			OFI responses (mm)		
ID #	x1	x2	x3	x4	x5	x6	x7	x8	x9	FP	DS	SW	FP	DS	SW
74	0.250	0.063	0.083	0.235	0.927	−8.990	28.08	14.85	109.6	57.82	37.70	13.87	53.42	36.12	13.44
75	0.088	−0.134	−0.250	−0.240	1.235	7.374	25.66	15.13	125.2	52.60	36.74	11.55	50.90	35.50	9.04
76	0.043	0.169	0.109	−0.210	1.083	9.192	59.60	15.70	72.9	57.54	40.84	8.92	83.94	62.53	10.44
77	0.109	−0.154	0.018	−0.063	1.013	7.778	33.33	16.21	112.4	47.64	34.13	9.80	50.69	35.40	6.94
78	−0.033	−0.053	−0.199	0.220	1.048	−1.515	56.77	14.68	70.2	62.49	40.96	9.70	69.70	47.53	5.06
79	−0.139	−0.043	−0.098	0.018	0.922	−7.374	29.70	14.83	93.1	54.92	37.79	10.94	59.88	38.01	11.50
80	−0.078	−0.184	0.210	−0.159	0.836	−1.717	45.45	15.15	104.1	75.69	53.28	12.14	75.69	53.28	12.14
81	−0.149	−0.023	−0.194	−0.119	1.124	1.515	36.97	15.02	115.1	46.55	34.73	7.94	67.68	53.70	6.30
82	0.235	0.250	−0.240	−0.104	0.826	−9.798	59.19	15.72	47.2	65.94	44.42	10.92	84.12	59.03	7.41
83	0.028	0.194	0.038	−0.068	0.917	0.707	55.56	15.49	51.8	62.60	41.44	9.49	81.49	56.11	7.48
84	0.215	0.215	0.124	−0.018	0.987	−5.354	58.79	16.70	116.9	48.45	36.35	9.68	75.51	48.96	6.26
85	−0.199	−0.068	−0.043	0.215	1.018	9.596	40.61	15.07	135.3	63.04	41.05	15.74	68.18	47.76	7.38
86	−0.159	−0.225	0.088	0.058	1.174	8.990	44.65	15.45	95.8	79.62	55.91	10.56	73.95	51.89	6.08
87	0.184	0.048	−0.033	−0.073	1.240	7.576	21.21	14.98	54.6	58.34	38.24	12.94	54.13	32.75	13.68
88	−0.013	0.013	−0.139	−0.028	0.957	6.970	32.12	15.94	69.2	67.05	46.38	8.49	68.88	49.86	6.32
89	0.093	−0.144	−0.008	0.149	1.149	4.545	49.49	15.79	87.6	54.86	40.37	12.17	76.24	57.80	6.42
90	0.119	−0.149	−0.129	−0.013	0.876	7.172	23.64	16.51	96.8	52.31	36.39	12.47	52.31	36.39	12.47
91	−0.088	0.078	−0.154	0.169	1.230	−5.556	21.62	15.51	64.7	58.42	36.68	13.35	53.12	33.81	12.95
92	0.033	−0.038	−0.149	0.023	0.785	0.303	37.78	15.58	73.8	69.16	46.56	11.90	75.77	52.59	6.78
93	0.104	0.184	0.033	−0.093	0.750	−0.101	47.07	15.87	71.1	72.49	51.98	8.51	74.21	47.12	7.26
94	−0.164	−0.088	−0.013	0.179	0.806	−0.909	30.51	15.28	89.4	74.33	50.40	14.50	63.64	43.43	13.65
95	0.058	−0.098	−0.174	−0.144	1.154	−9.394	34.55	14.66	117.9	50.52	35.43	10.27	57.94	44.29	5.55
96	−0.083	0.083	0.098	0.199	0.972	2.121	41.82	15.00	53.7	62.13	37.85	12.31	80.96	61.84	7.09
97	−0.098	−0.013	−0.134	−0.194	1.098	4.343	25.25	15.34	65.6	60.06	39.80	9.47	61.67	41.69	8.33
98	−0.215	0.154	−0.179	−0.129	1.073	4.747	52.73	16.19	133.4	50.34	35.95	7.09	49.00	37.07	6.85
99	0.003	0.139	0.119	−0.098	0.871	0.505	38.18	14.64	118.8	59.72	39.42	15.27	67.57	45.88	9.69
100	−0.038	−0.093	0.028	−0.043	0.932	−5.758	20.40	14.90	105.9	54.47	33.03	18.10	36.77	23.46	13.33

Table A2. Test points and corresponding responses (intrusion distances) for both crash scenarios.

	Input variables									FFI responses (mm)			OFI responses (mm)		
ID #	x1	x2	x3	x4	x5	x6	x7	x8	x9	FP	DS	SW	FP	DS	SW
1	0.051	−0.161	0.138	0.232	1.062	0.637	39.04	16.32	90.5	63.40	42.91	12.12	68.02	43.95	8.88
2	−0.183	0.182	−0.184	0.078	0.863	−0.325	31.83	15.83	58.2	62.99	38.13	12.44	75.36	55.38	4.06
3	0.206	0.081	0.010	0.205	0.807	5.986	39.75	15.53	68.0	62.32	43.71	11.77	62.89	39.34	12.80
4	0.229	0.032	−0.159	0.055	0.903	9.024	55.31	15.02	89.6	59.08	41.82	9.64	60.81	47.70	10.67
5	0.041	−0.127	0.085	−0.166	0.838	2.611	27.81	15.00	93.2	68.34	46.20	13.20	69.04	48.31	9.82
6	−0.102	−0.194	−0.068	−0.149	0.953	2.811	34.13	16.40	91.8	68.37	45.58	13.02	65.04	47.72	11.53
7	−0.169	0.065	0.048	−0.233	1.242	0.899	20.38	15.69	52.1	57.85	35.34	15.66	75.07	49.19	6.43
8	−0.177	0.046	−0.135	0.233	0.911	−1.710	26.26	15.44	102.7	65.71	36.80	14.76	59.09	40.68	13.01
9	−0.118	−0.074	−0.155	0.087	0.836	4.064	24.06	16.34	76.2	64.14	41.27	14.70	58.24	38.14	14.37
10	−0.108	0.231	−0.201	0.084	1.038	0.723	49.15	15.05	107.8	53.97	37.84	8.30	59.77	35.76	13.78
11	−0.086	−0.145	0.022	0.020	1.081	−4.583	42.70	15.82	126.9	50.11	37.99	9.58	62.29	42.51	11.64
12	0.182	−0.041	0.216	−0.205	0.812	3.470	49.56	15.09	102.9	61.17	43.68	8.68	67.20	41.91	10.84
13	0.108	0.038	0.215	−0.157	1.091	8.105	54.38	14.87	97.6	54.63	39.44	9.36	66.96	46.16	8.11
14	−0.017	0.188	0.147	−0.219	0.962	5.900	31.61	15.15	85.8	68.57	43.27	11.08	64.14	50.88	9.50
15	−0.003	−0.175	0.155	−0.126	1.085	3.604	36.38	16.39	123.8	54.13	32.72	11.83	81.25	56.20	8.65
16	0.037	0.174	0.089	0.047	1.157	0.979	42.59	16.37	52.5	59.21	44.66	11.98	72.22	57.24	6.79
17	−0.070	−0.039	0.059	−0.077	1.125	1.286	59.68	16.61	108.2	49.73	32.07	9.86	67.81	46.06	10.08
18	−0.143	−0.114	0.187	0.097	0.896	1.585	39.40	15.23	101.2	58.68	40.24	15.12	84.79	59.72	6.96
19	−0.154	−0.068	−0.058	0.219	0.786	−3.197	54.49	16.21	114.5	62.52	42.10	12.67	64.14	43.92	9.15
20	0.183	0.146	0.173	−0.040	0.798	3.262	35.54	15.23	100.1	52.53	42.44	12.03	79.60	48.97	5.63
21	0.085	0.249	−0.054	−0.029	1.065	−4.939	56.43	15.55	85.8	59.45	42.38	8.68	69.86	49.23	6.76
22	−0.026	−0.102	0.078	0.171	0.985	5.158	39.17	14.97	92.9	65.01	43.88	13.57	76.60	59.32	7.48
23	0.082	0.032	0.061	−0.145	0.948	−0.821	23.96	15.34	87.3	55.43	36.46	15.20	64.37	40.47	10.98
24	−0.178	0.037	−0.114	0.210	1.199	1.512	50.36	16.36	114.0	61.50	46.74	10.07	82.11	52.42	6.88
25	−0.132	0.056	0.051	0.221	1.013	9.005	43.55	15.80	96.2	55.19	38.01	10.90	62.39	40.97	10.71
26	−0.208	−0.079	−0.018	0.027	0.828	−4.313	29.06	14.90	76.2	74.02	49.19	12.92	67.57	51.91	6.00
27	0.010	0.116	0.071	−0.059	0.858	−7.063	47.17	15.98	69.2	73.79	50.33	8.25	81.87	57.95	6.14
28	0.240	0.176	−0.207	0.165	1.042	6.245	56.76	15.97	70.9	54.07	36.25	11.12	70.83	46.37	6.98
29	0.216	−0.093	−0.236	0.087	0.900	2.468	57.68	15.01	103.6	48.91	34.78	9.86	52.73	33.51	13.18
30	−0.006	−0.102	−0.169	−0.058	0.780	−6.103	20.97	15.42	86.8	57.90	35.83	16.99	58.61	40.75	11.29
31	0.182	−0.230	−0.149	−0.122	1.226	−0.069	55.66	16.46	67.5	50.39	36.44	11.61	68.93	48.54	6.62
32	0.155	0.043	−0.229	−0.070	1.100	8.080	51.61	15.25	80.2	64.37	45.74	9.48	65.53	44.24	13.79
33	0.107	0.160	−0.071	0.170	0.813	1.747	42.62	14.89	118.3	55.44	34.31	13.09	75.61	47.15	5.56
34	0.107	0.142	0.002	0.088	1.091	8.569	40.23	15.03	124.2	52.17	39.65	10.57	77.68	56.16	7.61
35	0.007	0.106	−0.117	0.059	1.095	2.197	59.63	16.18	67.2	55.78	42.03	9.57	76.66	55.18	6.30
36	0.220	−0.080	−0.229	−0.184	0.801	2.143	41.26	15.75	123.2	53.06	30.78	13.02	74.74	45.72	5.34
37	−0.208	−0.243	−0.106	−0.005	1.138	8.822	54.65	16.36	98.6	70.61	51.39	9.20	45.35	34.43	16.62
38	−0.094	0.004	−0.087	0.226	0.948	2.163	35.93	16.18	46.8	65.64	47.96	14.28	67.99	56.13	9.21
39	−0.033	0.169	−0.204	0.186	0.960	7.863	58.47	15.29	49.8	57.20	41.15	11.64	86.93	66.72	8.79
40	−0.196	0.194	0.223	0.192	1.015	7.312	37.66	15.04	107.8	52.52	33.23	16.50	66.29	44.45	9.83